Article

Neuron

Cortical Feedback Regulates Feedforward Retinogeniculate Refinement

Highlights

- V1 activity was chronically disrupted during the thalamic critical period
- Suppressing V1 led to the recruitment of additional RGC inputs onto relay neurons
- Increasing L6 firing also led to rewiring, implying an instructive role for feedback
- Manipulating V1 after the thalamic critical period no longer triggered RGC rewiring

Authors

Andrew D. Thompson, Nathalie Picard, Lia Min, Michela Fagiolini, Chinfei Chen

Correspondence

chinfei.chen@childrens.harvard.edu

In Brief

Thompson et al. show that, contrary to the traditional "feedforward" model of sensory pathway development, feedback from L6 of V1 influences experience-dependent refinement of retinogeniculate projections. Their findings indicate that thalamus and cortex interact bidirectionally during development to fine-tune visual circuits.

Thompson et al., 2016, Neuron *91*, 1021–1033
September 7, 2016
http://dx.doi.org/10.1016/j.neuron.2016.07.040

CellPress

Neuron
Article

Cortical Feedback Regulates Feedforward Retinogeniculate Refinement

Andrew D. Thompson,[1,2] Nathalie Picard,[2] Lia Min,[2,3] Michela Fagiolini,[2,3] and Chinfei Chen[2,3,*]
[1]BBS Program, Harvard Medical School, 220 Longwood Avenue, Boston, MA 02115, USA
[2]Department of Neurology, F.M. Kirby Neurobiology Center, Boston Children's Hospital, 300 Longwood Avenue, Boston, MA 02115, USA
[3]Program in Neuroscience, Harvard Medical School, 220 Longwood Avenue, Boston, MA 02115, USA
*Correspondence: chinfei.chen@childrens.harvard.edu
http://dx.doi.org/10.1016/j.neuron.2016.07.040

SUMMARY

According to the prevailing view of neural development, sensory pathways develop sequentially in a feedforward manner, whereby each local microcircuit refines and stabilizes before directing the wiring of its downstream target. In the visual system, retinal circuits are thought to mature first and direct refinement in the thalamus, after which cortical circuits refine with experience-dependent plasticity. In contrast, we now show that feedback from cortex to thalamus critically regulates refinement of the retinogeniculate projection during a discrete window in development, beginning at postnatal day 20 in mice. Disrupting cortical activity during this window, pharmacologically or chemogenetically, increases the number of retinal ganglion cells innervating each thalamic relay neuron. These results suggest that primary sensory structures develop through the concurrent and interdependent remodeling of subcortical and cortical circuits in response to sensory experience, rather than through a simple feedforward process. Our findings also highlight an unexpected function for the corticothalamic projection.

INTRODUCTION

Sensory circuits develop through the initial formation of an imprecise connectivity that subsequently refines with experience. The quintessential example of this process is the experience-dependent rewiring of connections in the visual cortex that occurs during critical periods of plasticity (Katz and Shatz, 1996; Wiesel and Hubel, 1963). This sensory-dependent rewiring of neuronal connections has traditionally been considered a hallmark of cortical circuits, as those in the retina and thalamus were thought to mature before eye opening. However, recent reports have demonstrated that subcortical structures are also shaped by experience and that this plasticity extends relatively late in postnatal development. In mice, neuronal circuits in the retina, visual thalamus, and somatosensory thalamus all exhibit sensitivity to sensory experience during time windows that overlap with critical periods in corresponding primary sensory cortices (Dunn et al., 2013; Gordon and Stryker, 1996; Hooks and Chen, 2006; Tian and Copenhagen, 2003; Wang and Zhang, 2008). While it has become clear that peripheral structures are also shaped by experience, the fact that cortical and subcortical circuits mature concurrently raises the question of whether cortex exerts influence on subcortical experience-dependent refinement.

In the visual pathway, the retinogeniculate synapse, the connection between retinal ganglion cells (RGCs) and thalamic relay neurons in the dorsal lateral geniculate nucleus (dLGN) has served as a powerful model for studies of early synaptic refinement. In mice, development at this synapse entails multiple phases that span the first month of postnatal life (Hong and Chen, 2011). The first two phases are driven by molecular cues and spontaneous activity and involve the pruning and strengthening of RGC inputs to establish a rough draft of the mature circuit by postnatal day (P20) (Chen and Regehr, 2000; Huberman et al., 2008; Sretavan and Shatz, 1984). Refinement of this draft then becomes dependent on visual experience during a thalamic critical period that occurs between P20 and P30. Visual deprivation at this time (which we refer to as late dark rearing [LDR]) leads to a dramatic rewiring of the circuit as additional weak RGC inputs are recruited to innervate each thalamic relay neuron (Hooks and Chen, 2006, 2008).

These observations suggest that sensory input from retina fine-tunes and stabilizes the adult pattern of connectivity in thalamus. In contrast to the LDR paradigm, dark rearing from birth (chronic dark rearing, CDR) does not trigger retinogeniculate rewiring in spite of the (continued) visual deprivation from P20 to P30 (Hooks and Chen, 2006, 2008; Lin et al., 2014). It is important to note here that the experience-dependent phase of retinogeniculate development overlaps with critical periods in primary visual cortex (V1), which also requires visual experience to develop normally (Fagiolini et al., 1994; Gordon and Stryker, 1996; Kang et al., 2013). Thus, it is possible that the distinct retinogeniculate responses to LDR versus CDR may be related to the level of maturation of visual cortex.

While the retinal input transmits primary visual information to relay neurons, the majority of glutamatergic synapses onto these cells arise from corticothalamic neurons residing in layer 6 (L6) of primary visual cortex (V1) (Guillery and Sherman, 2002; Montero, 1991). L6 corticothalamic cells modulate relay neuron firing in the adult via this direct, excitatory projection as well as through disynaptic inhibitory pathways (Figure 1A) (Crandall

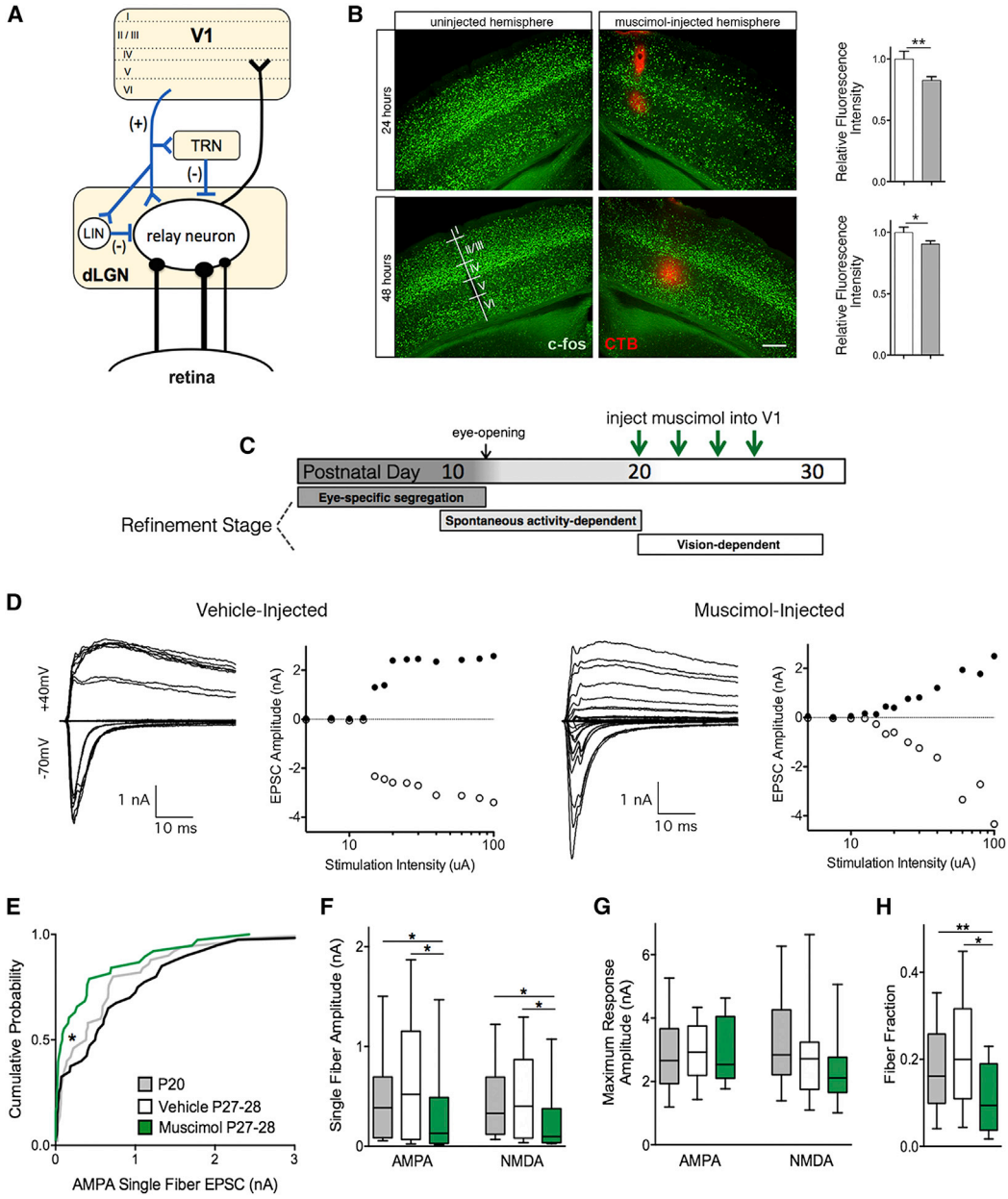

Figure 1. Disrupting Activity in V1 with Muscimol between P20 and P27 Alters Connectivity of the Retinogeniculate Synapse

(A) Schematic of the primary visual pathway. The feedforward pathway projections are colored in black, the feedback pathway in blue. (+) indicates excitatory synapses, (–) indicates inhibitory synapses. TRN, thalamic reticular nucleus; LIN, local inhibitory neuron.

(B) Immunohistochemistry reveals that expression of the activity-dependent marker c-*fos* is reduced unilaterally in V1 both 24 and 48 hr after muscimol injection (injection tract marked by red CTB n = 5 sections, 3 mice for each time point; scale bar, 200 μm). Quantification (right) shows mean ± SEM.

(C) Schematic depicting experimental design.

(D) Example recordings from relay neurons of vehicle- or muscimol-injected mice. Each graph shows overlaid AMPAR-mediated (inward currents, recorded at −70 mV) and AMPA- and NMDAR-mediated (outward currents, recorded at +40 mV) EPSCs evoked by incrementally increasing optic tract stimulation. To the right of overlaid traces, peak EPSC amplitudes for the traces shown are plotted by stimulus intensity.

(E) Cumulative probability plot of AMPAR-mediated single fiber EPSCs shows a significant shift toward weaker retinal inputs in muscimol-treated mice.

(F) AMPAR- and NMDAR-mediated single-fiber strengths were significantly reduced after muscimol injections, as compared with younger mice (P20, gray) as well as vehicle-injected age-matched littermates (white).

(G) Maximal EPSCs were not significantly altered.

(H) The average number of retinal inputs innervating each relay neuron increased after 1 week of muscimol injections, indicated by the decreased fiber fraction. For (E)–(H), box plots show interquartile range, whiskers show 10th and 90th percentiles. n = P20: 30 cells from 6 mice; vehicle injected: 25 cells from 4 mice; muscimol injected: 20 cells from 4 mice; *p < 0.05, **p < 0.01.

et al., 2015; Guillery and Sherman, 2002). Notably, development of the corticothalamic projection is delayed relative to retinal inputs, only completing innervation of the dLGN after eye opening (Seabrook et al., 2013; Jacobs et al., 2007; Shatz and Rakic, 1981). Corticogeniculate inputs then strengthen functionally during the second phase of retinogeniculate refinement (Jurgens et al., 2012), just prior to onset of experience-dependent retinogeniculate rewiring. This developmental sequence raises the question: does cortical feedback influence vision-dependent remodeling of retinothalamic connectivity? Here we test this possibility by examining the effects of manipulating cortical activity during development on refinement of the retinogeniculate circuit. Our results show that distinct manipulations of cortical activity patterns all result in a retinogeniculate rewiring response marked by the recruitment of additional retinal inputs onto each relay neuron, similar to that observed after LDR. Our findings suggest that postnatal development entails a critical period during which bidirectional interactions between thalamus and cortex guide the remodeling and consolidation of their constituent synaptic networks.

RESULTS

Pharmacological Disruption of Visual Cortical Activity Alters Retinogeniculate Refinement

The defining feature of the retinogeniculate response to LDR (late dark rearing) is an increase in the number of functional afferent inputs onto relay neurons (Hooks and Chen, 2006). To assess whether a change in cortical activity can elicit a similar retinogeniculate response, we delivered the $GABA_AR$ agonist muscimol to V1 unilaterally via stereotactic injection. This manipulation significantly reduced immunostaining for the protein product of the immediate early gene *c-fos* throughout V1 when compared to the uninjected hemisphere at both 24 and 48 hr after injection, indicating that a single muscimol injection disrupted activity in V1 for up to 2 days (see Experimental Procedures; Figure 1B). Therefore, we injected mice with either muscimol or saline control during the thalamic critical period (beginning at P20 and again every 48 hr thereafter until P27–P28), after which we prepared acute brain slices of the dLGN and characterized retinogeniculate connectivity via whole-cell patch-clamp recordings from relay neurons (Figure 1C).

To quantify retinogeniculate connectivity, we recorded excitatory synaptic currents from relay neurons evoked by optic nerve stimulation with incrementally increasing intensity. Figure 1D shows representative examples of AMPAR- and NMDAR-mediated synaptic currents recorded from a saline-injected (left) and muscimol-injected (right) mouse. In both examples, synaptic currents increase in amplitude as increasing stimulus intensities recruit additional presynaptic RGC axons; however, there are many more "steps" in the muscimol-treated compared with the saline-treated mouse. We quantified the difference in connectivity by measuring the single fiber strength (the amplitude of an EPSC evoked by minimal stimulation) and the maximal response (the amplitude of an EPSC evoked by activating all intact retinal inputs to the recorded neuron) as previously described (see Experimental Procedures and Hooks and Chen, 2008). After disrupting cortical activity with one week of muscimol injections, the average single fiber strength was reduced compared to saline-injected controls by more than 70% ($p < 0.05$, < 0.05 for AMPAR and NMDAR EPSCs, Mann-Whitney [MW] test; Figures 1E and 1F and Table S1), while maximal currents were not significantly affected (Figure 1G).

To estimate the convergence of RGCs onto relay neurons, we calculate the fiber fraction, the contribution of a single retinal input to the total retinal drive onto a relay neuron (amplitude of single fiber EPSC/maximal EPSC; see Experimental Procedures and Hooks and Chen, 2006). The inverse of this fraction provides a rough estimate of the number of retinal inputs that innervate a single relay neuron, and averaging the fiber fraction of a population of relay neurons allows quantitative comparison of the refinement state in different conditions, when the number of inputs is too great to reliably count as stepwise increments in amplitude. We found that disrupting activity in visual cortex with muscimol injections from P20 to P27 reduced the fiber fraction at the retinogeniculate synapse by 50% ($p < 0.05$, MW; Figure 1H), demonstrating altered refinement of the retinothalamic circuit in response to the change in cortical activity.

The reduction in fiber fraction observed in muscimol-injected mice at P27 compared with saline-injected control mice could represent a failure to further refine the connection between P20 and P27 or the recruitment of additional retinal afferents during the experience-dependent phase of retinogeniculate development (as observed in LDR). To distinguish between these two possibilities, we also performed LGN recordings from untreated mice at P20. Results obtained from these experiments showed that the fiber fraction in muscimol-injected mice decreased between P20 and P27, indicative of new presynaptic partners forming synapses onto relay neurons during this time window ($p < 0.01$, MW with Holm-Bonferroni correction; Figure 1H). These changes were driven by a decrease in the single fiber strength ($p < 0.05$, AMPA, < 0.05, NMDA, MW with Holm-Bonferroni correction; Figures 1E–1H), demonstrating that disrupting cortical feedback during the experience-dependent stage of retinogeniculate remodeling causes a rewiring response in which newly functional, weak retinogeniculate connections are added to the circuit.

Disrupting Cortical Feedback Induces Rewiring in Ipsilateral LGN, but Not Contralateral LGN

Our findings with muscimol strongly suggested that the corticothalamic pathway (by which we refer to both the direct, excitatory projection and disynaptic inhibitory pathways) contributes to the refinement of the retinogeniculate projection. However, the diffusion of muscimol within the brain is difficult to quantify directly, and the possibility remained that the drug was diffusing into the ventricles and circulating throughout the brain via the cerebrospinal fluid. In order to rule out that muscimol injected into V1 reaches the CSF and acts at LGN directly, we repeated the muscimol experiment, injecting muscimol or saline control into V1 every 48 hr beginning at P20, and at P27–P28 characterized the retinogeniculate projection in the dLGN contralateral to the manipulated hemisphere. Results from these experiments showed no difference in single fiber strength, maximal currents, or fiber fraction of muscimol versus vehicle-injected mice, confirming that disrupting activity in V1 during development alters

retinogeniculate refinement only in the ipsilateral LGN targeted by the corticothalamic projection (Figure S1).

Disrupting L6 Activity in V1 with HM4Di Also Triggers Retinogeniculate Remodeling

To further expand on this finding, we sought an alternative approach to chronically manipulate the activity of L6 corticothalamic neurons. To this end, we employed DREADD (designer receptors activated exclusively by designer drugs) technology—modified G protein-coupled receptors that respond only to the biologically inert ligand clozapine-N-oxide (CNO). Previous studies have shown that activation of the inhibitory DREADD receptor, HM4Di, by CNO can trigger hyperpolarization of neurons through modulation of inward rectifying K^+ (GIRK) channels (Armbruster et al., 2007). We combined DREADD technology with the transgenic mouse line NTSR1-Cre (GENSAT220, RRID: MGI_5304490) (Gong et al., 2007), which expresses Cre recombinase specifically in L6 corticothalamic neurons (Bortone et al., 2014). Injection of adeno-associated virus encoding a Cre-dependent form of the inhibitory DREADD HM4Di (AAV8-hSyn-DIO-HM4Di-mCherry) into V1 of neonatal NTSR1-Cre mouse pups yielded strong expression of HM4Di selectively in L6 cells by P20 (Figure 2A). Terminal projections from labeled corticothalamic neurons could also be visualized in the dLGN (Figure 2B). To assess the efficacy of the HM4Di receptor in L6 neurons, we performed current-clamp recordings from cortical slices taken from these mice. Both resting membrane potential and the firing rates evoked with depolarizing current steps were significantly reduced during bath application of CNO, consistent with hyperpolarization and decreased excitability of corticothalamic neurons upon activation of HM4Di (Figure 2C). Furthermore, when we recorded corticothalamic synaptic currents in relay neurons in LGN slices from NSTR1-Cre mice expressing HM4Di, we found that application of CNO lead to a decrease in the EPSC amplitude, as well as an increase in paired-pulse ratio, indicating a reduction in probability of release at the terminals of L6 cells (Figure S2). Therefore, HM4Di reduced L6 neuronal activity and neurotransmitter release, as reported previously (Armbruster et al., 2007; Stachniak et al., 2014).

To confirm the efficacy of HM4Di in manipulating the activity of L6 cells chronically in the intact brain, we conducted in vivo recordings in anesthetized NTSR1-Cre mice expressing HM4Di injected with CNO twice a day from P20 to the day of recording (P32–P35; see Experimental Procedures). We used 16-channel linear probes to record visual activity in V1. To evaluate the laminar location of each recording site, we first recorded local field potentials in response to contrast-reversing square checkerboard (Figures S3A and S3B). After measuring baseline visually evoked and spontaneous activity of pyramidal cells across all cortical layers, we administered CNO systemically and assessed changes in activity over time. Results showed that both evoked and spontaneous L6 activity were significantly reduced after CNO administration ($p < 0.01$ for both; Friedman test with Dunn's multiple comparisons test; Figure 2F). In addition, evoked activity in L4 and superficial layers significantly increased after CNO injection ($p < 0.0001$; Figures 2G and 2H), consistent with the "gain control" model recently proposed for the role of L6 in the cortical column, whereby suppression of L6 disinhibits activity in superficial layers (Bortone et al., 2014; Olsen et al., 2012). Interestingly, when we compared the baseline visual response at P30 after chronic CNO treatment from P20 (just before the next CNO injection), we found that evoked activity in L4 was lower, suggesting a compensatory change in L4 activity after prolonged activation of HM4Di in L6 ($p < 0.05$; Kruskal-Wallis with Dunn's multiple comparisons test; Figure S3).

We next examined the effects of chronic HM4Di-mediated perturbation of cortical activity on retinogeniculate refinement (Figure 3A). LGN slices were prepared at P27–P33 and screened for diffuse fluorescence in dLGN to confirm viral expression before recording. HM4Di expression was observed in corticothalamic axon fibers but never directly in relay neurons (Figure S4). Representative examples of recordings from these mice are shown in Figure 3B. As with muscimol injections, HM4Di-mediated suppression of L6 activity led to a significant reduction in fiber fraction when compared to vehicle-injected HM4Di-positive control mice (48.5% decrease; $p < 0.01$, MW; Figure 3F) and to CNO-treated control mice lacking HM4Di ($p < 0.01$; Figure S5). In contrast to results from muscimol-injected mice, single fiber strengths were not significantly altered (Figures 3C and 3D), while maximal currents were instead markedly increased (AMPAR EPSC by 37.3%, $p < 0.01$; NMDAR EPSC by 76.8%, $p < 0.001$; Figure 4E). In response to both manipulations, additional retinal inputs are recruited into the circuit, but in the case of HM4Di-mediated inhibition, the new inputs also strengthen. This finding is not altogether surprising, as previous work has shown changes in retinal input strength and number are dissociable in response to different visual manipulations (Lin et al., 2014). These results demonstrate that distinct alterations in cortical activity can mediate different effects on the plasticity of RGC inputs.

HM4Di-Mediated Suppression of L6 Leads to Elevated Activity Levels in dLGN Relay Neurons

To further understand the functional consequences of L6 manipulation with HMD4i, we performed in vivo recordings from the dLGN of NTSR1-Cre mice at P30–P35 after chronic activation of HM4Di in L6 from P20. To confirm proper placement of the electrode, brains were sectioned after recordings, and the electrode tract was identified. In a subset of experiments, electrodes were coated with DiO to better visualize the recorded site (Figure 4A). Visual responses to drifting gratings were recorded approximately 6 hr after a CNO injection. The spontaneous activity of all units recorded trended higher in CNO-treated mice but was not significantly different from that of control mice (Figure 4B). Next, as LGN neurons display different features of visual responsiveness (Piscopo et al., 2013), we classified the units recorded in vivo as non-responsive (no effect induced by our visual stimulation), visually responsive (increased activity induced by visual stimulation), or suppressed cells (decreased activity induced by visual stimulation). We found a significant shift toward more visually activated cells and fewer visually suppressed cells after chronic CNO treatment in comparison with vehicle control mice ($p < 0.01$, chi-square test; Figure 4C). Finally, within the visually activated cell population, the maximal evoked response was 2-fold higher in CNO-treated mice compared with saline-injected controls ($p < 0.01$; Figure 4D).

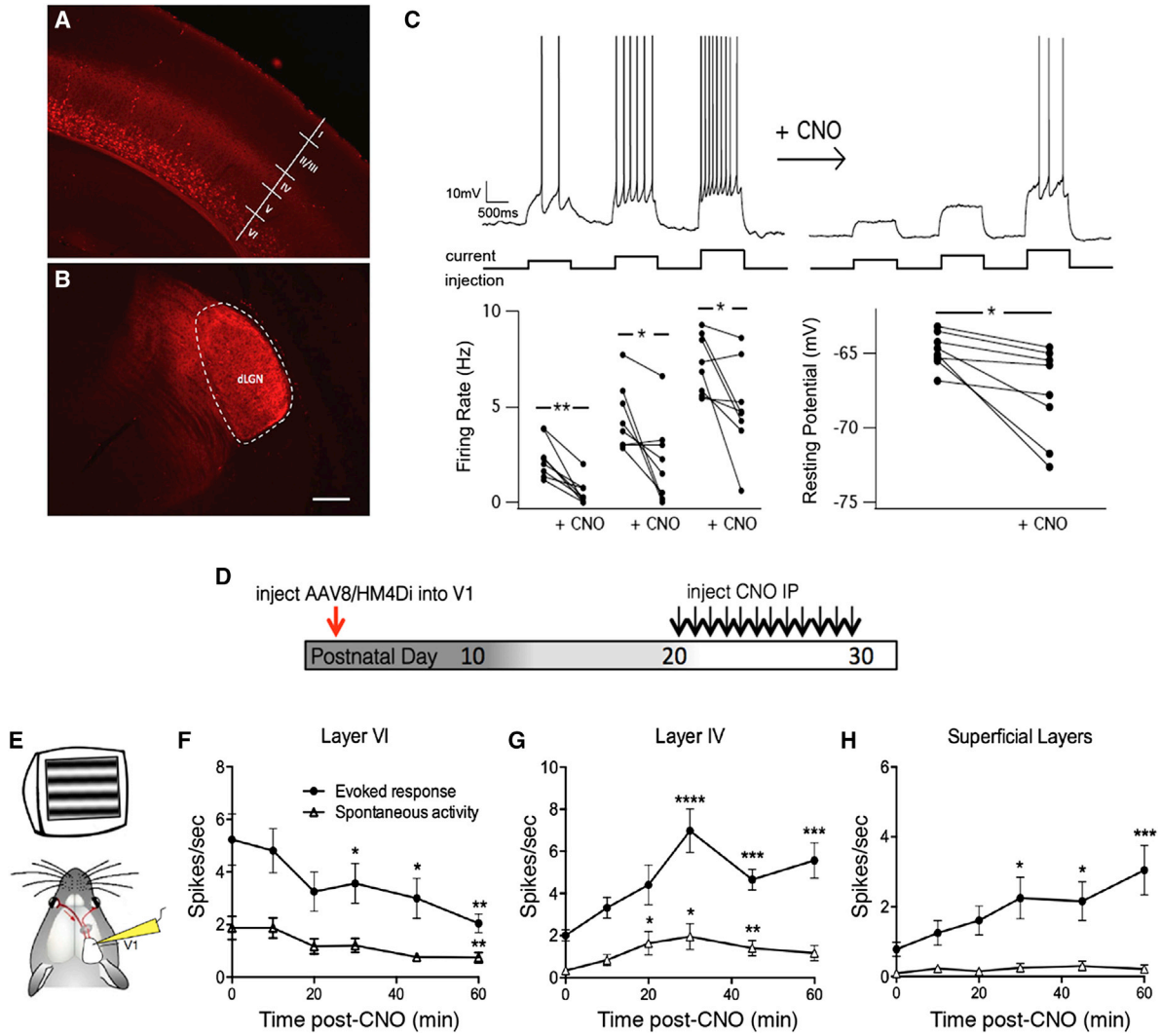

Figure 2. The Inhibitory DREADD HM4Di Can Suppress L6 Corticothalamic Cells

(A) mCherry expression labels L6 somas in a P20 NTSR1-Cre mouse injected neonatally with AAV2/8-hSyn-DIO-HM4Di-mCherry.

(B) Diffuse mCherry fluorescence from corticothalamic axons is visible in the dLGN. Scale bar, 200 μm.

(C) Current-clamp recordings of L6 cells expressing HM4Di show a robust hyperpolarization and reduction in firing rates upon application of CNO (n = 8 cells from 8 slices).

(D) Schematic depicting experimental design for chronic manipulation of L6 activity during the critical period.

(E) Schematic of in vivo recording approach.

(F) Pyramidal cells recorded from L6 cells of NTSR1-Cre mice expressing HM4Di show decreased firing within 30 min after i.p. injection of CNO (n = 25 cells from 6 mice; Friedman test with Dunn's multiple comparison test to assess changes longitudinally).

(G) Activity of L4 pyramidal cells in NTSR1-Cre mice expressing HM4Di shows significantly increased firing 30 min after i.p. injection of CNO, consistent with a suppressed output from L6 cells (n = 21 cells).

(H) Pyramidal cells in superficial layers also increased firing after CNO injection (n = 10 cells).

Error bars in (F)–(H) denote SEM.

Increasing L6 Activity with HM3Dq Also Induces Retinogeniculate Rewiring

Taken together, our results demonstrate that suppressing cortical feedback can alter feedforward retinogeniculate refinement, leading to an increase in the number of functional afferents innervating each relay neuron. This same change in connectivity occurs when mice are dark-reared from P20. Therefore, we next questioned whether this rewiring occurs in response to a loss of feedback or to a change in feedback. To distinguish between these two scenarios, we manipulated the activity of L6 cells in NTSR1-Cre mice by injecting virus encoding HM3Dq (AAV8-hSyn-DIO-HM3Dq-mCherry), which increases neuronal firing via the canonical Gq pathway (Alexander et al., 2009). We reasoned that this manipulation would disrupt the coding of visual information returning from cortex via L6, but without reducing activity. Importantly, the excitatory effect of HM3Dq

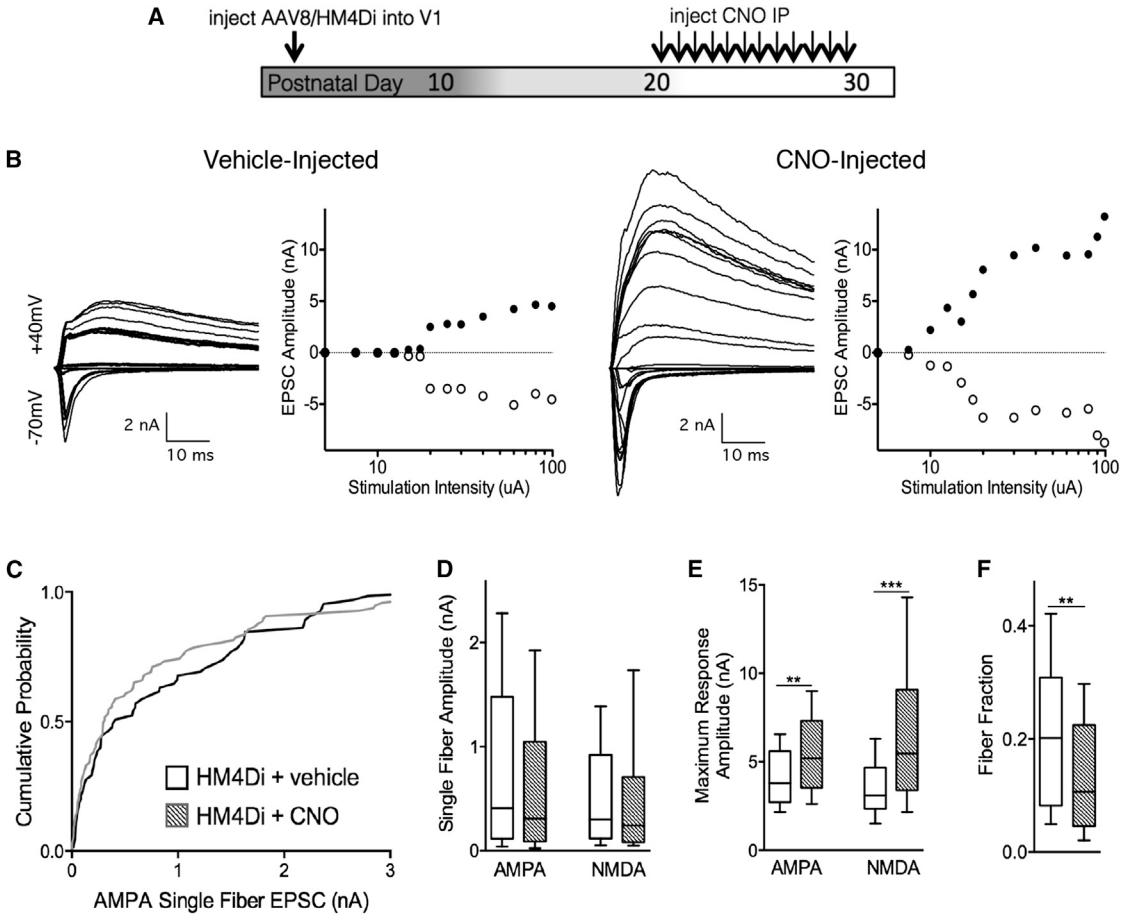

Figure 3. HM4Di-Mediated Suppression of L6 Induces the Recruitment of Additional, Strong Retinal Inputs onto Relay Neurons

(A) Schematic depicting experimental design.

(B) Example recordings from relay neurons of NTSR1-Cre mice expressing HM4Di, injected with vehicle or CNO from P20 to P27–P33. EPSC amplitudes plotted by stimulus intensity again show few discrete steps in the control example and more steps in the cell from a CNO-injected mouse.

(C) Cumulative probability plot of AMPAR-mediated single fibers shows no shift in the strength of retinal inputs in CNO-injected mice.

(D) Neither AMPAR- nor NMDAR-mediated single fiber strength was altered by suppressing L6 with HM4Di.

(E) Both AMPAR- and NMDAR-mediated maximum EPSCs were increased after CNO injections.

(F) The number of retinal inputs converging on each relay neuron was significantly increased in mice injected with CNO.

For (C)–(F), box plots show interquartile range, whiskers show 10th and 90th percentiles. n = vehicle injected: 34 cells from 9 mice; CNO injected: 50 cells from 11 mice. **p < 0.01, ***p < 0.001.

on L6 neurons—as assessed by in vitro recordings—remained potent even after 7 days of activation in vivo, indicating that repeated activation did not lead to desensitization of the HM3Dq receptor or compromise cell health ($p < 0.01$, paired t test; Figure S6). We then assessed the effect of this manipulation on retinogeniculate refinement (Figures 5A and 5B). As with muscimol and HM4Di, slice recordings revealed a significantly reduced fiber fraction after DREADD activation ($p < 0.01$; Figure 5F). With increased corticothalamic activity, AMPA single fiber strength was reduced by 53.2% ($p < 0.05$, MW; Figures 5C and 5D), and NMDA single fiber strength trended lower ($p = 0.18$, MW; Figure 5D), while maximal currents did not change (Figure 5E). These results support the idea that abnormally elevated cortical feedback also disrupts retinogeniculate development. Thus, proper maturation of the retinogeniculate circuit does not simply require a threshold level of cortical feedback, but rewires in response to both increased and decreased activity of L6 corticothalamic cells.

Cortical Influence on Retinogeniculate Remodeling Is Constrained to the Thalamic Critical Period

We next asked whether the influence of cortical feedback on retinogeniculate connectivity persists throughout life, or if it is limited to the critical period. To address this question, we again used HM4Di to manipulate cortical feedback in NTSR1-Cre mice, injecting CNO or vehicle after closure of the thalamic critical period, from P30 until P37–P42 (Figure 6A; Hooks and Chen, 2008). Altering cortical feedback in this time window did not cause any significant changes in retinothalamic inputs. Single fiber strengths and maximal EPSCs remained constant (Figures

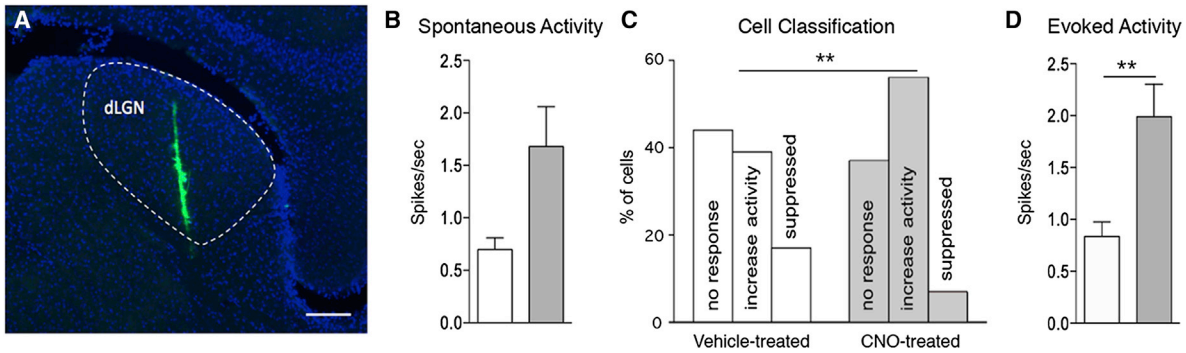

Figure 4. Chronic HM4Di-Mediated Suppression of L6 Cells in NTSR1-Cre Mice Leads to Increased Activity in dLGN Relay Neurons

(A) Recording site in dLGN labeled by DiO (green) painted on the electrode. LGN outlined by dashed lines. Cell nuclei are labelled by DAPI (blue). Scale bar, 200 μm.

(B) Spontaneous activity of relay neurons was not significantly affected by L6 suppression (n = 105 versus 133 cells from vehicle-treated [white] and CNO-treated [gray] mice).

(C) The distribution of relay neuron response profiles was significantly affected by chronic HM4DI-mediated L6 suppression.

(D) Evoked activity of visually responsive dLGN relay neurons was increased over 2-fold after 10 days of HM4DI-mediated suppression of L6 cells (n = 41 versus 75 cells; **$p < 0.01$).

Error bars in (B) and (D) represent SEM.

6B–6E). Most notably, in contrast to the same manipulation performed 10 days earlier, the fiber fraction was unchanged (Figure 6F). These findings indicate that retinogeniculate remodeling can respond to changes in cortical activity only during a period of development, after which retinothalamic circuitry is mature and less sensitive to alterations in feedback from V1.

DISCUSSION

The corticothalamic projection provides the largest glutamatergic input onto relay neurons in the dLGN, outnumbering retinal inputs by more than 4:1, yet its function in visual processing in the mature CNS remains a subject of active debate (Briggs and Usrey, 2008; Cudeiro and Sillito, 2006; Montero, 1991). Here we report a function for the corticothalamic projection that has not previously been considered: an influence on activity-dependent development of the retinogeniculate projection. We found that information relayed from cortex back to thalamus is critical for proper feedforward refinement of subcortical circuitry during the experience-dependent phase of retinogeniculate development. Three distinct manipulations of corticothalamic activity all triggered the recruitment of additional retinal inputs onto relay neurons. We propose that this configuration represents a common intermediate state of connectivity, from which a new retinothalamic wiring can be consolidated. Indeed, this connectivity resembles that triggered in mice dark-reared from P20, suggesting this is a common response to major changes in patterns of activity in the network.

A Revised Model for Developmental Retinogeniculate Refinement

Our working model for retinogeniculate development entails two early, spontaneous activity-dependent phases that set up an approximation of the final circuit (Figure 7). This feedforward circuit is functional even before eye opening, transmitting information to V1 (Ackman et al., 2012), while the feedback circuit does not fully innervate and strengthen until after eye opening (Jacobs et al., 2007). Then, after completion of the corticothalamic circuit, further fine-tuning and stabilization of the retinogeniculate connection occurs, mediated by sensory experience. Our results suggest there is a top-down regulation of this developmental process. The retinogeniculate remodeling that we observe here occurs in response to manipulations of cortical activity; we propose that in the course of normal development, visual experience and cortical feedback guide refinement in a more subtle fashion, without retinogeniculate connectivity fully reverting to the intermediate configuration. This model also provides an explanation for our previous observation that mice dark-reared from birth prune retinogeniculate inputs effectively, as chronic deprivation delays maturation of visual cortex (Fagiolini et al., 1994; Kang et al., 2013). In this condition, the circuit develops without meaningful feedback to remodel connections, and retinogeniculate inputs remain in their rough draft configuration that has not been optimized by experience.

A Developmental Function for Cortical Feedback

Results from our experiments suggest that remodeling of the retinothalamic circuit during the thalamic critical period depends strongly on cortically processed visual experience, fed back into the circuit via the corticothalamic projections. What is the function of this regulation during development? Corticothalamic feedback in the adult animal is arranged topographically and can synchronize or enhance relay neuron firing in response to specific stimuli (Murphy and Sillito, 1996; Sillito et al., 1994; Temereanca and Simons, 2004; Wang et al., 2006). The thalamic critical period may allow for the simultaneous rewiring of both glutamatergic projections onto relay neurons in order to establish proper alignment of retinal and cortical inputs, similar to the binocular

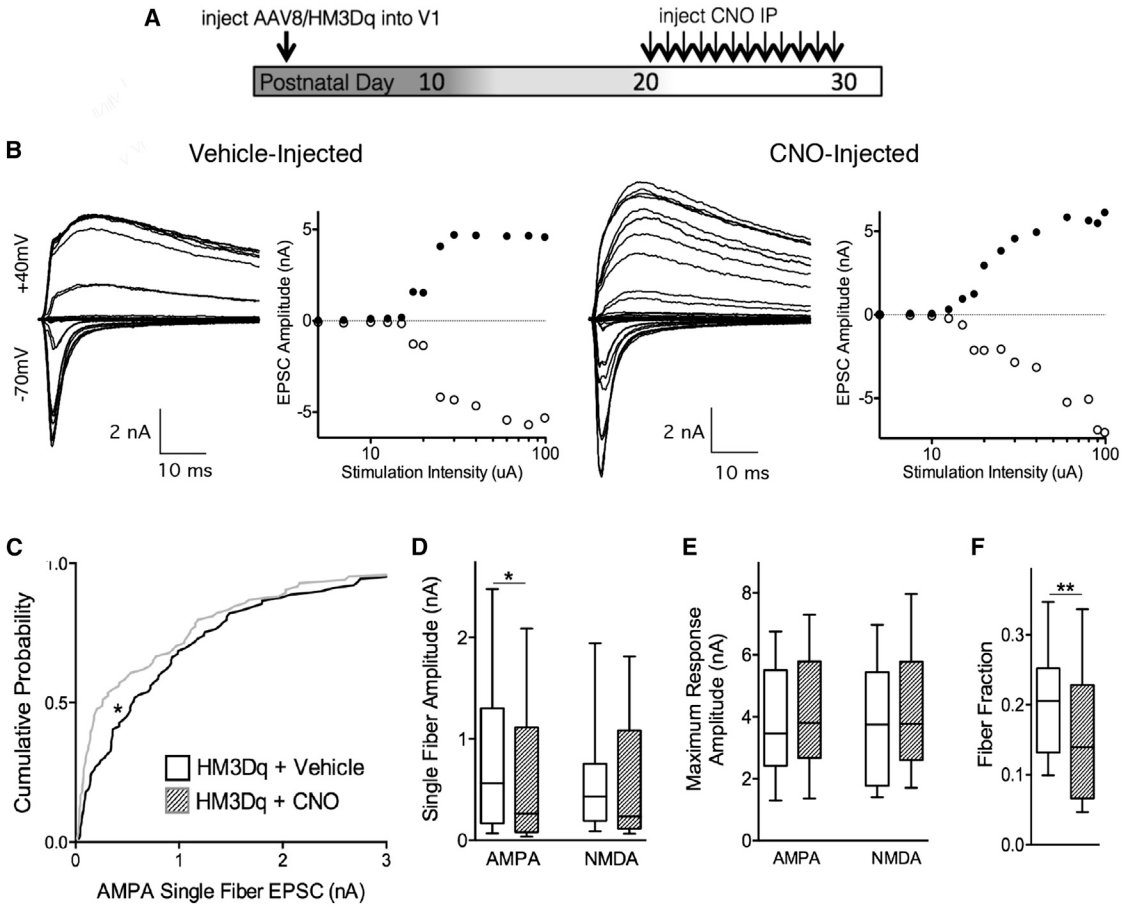

Figure 5. Enhancing L6 Neuronal Activity Also Triggers Remodeling of the Retinogeniculate Synapse

(A) Schematic depicting experimental design.

(B) Example recordings from relay neurons of NTSR1-Cre mice expressing HM3Dq, injected with vehicle or CNO from P20 to P27–P33.

(C) Cumulative probability plot of AMPAR-mediated single fibers shows a significant shift toward weaker retinal inputs in CNO-injected mice.

(D) AMPA- and NMDA-mediated single fiber strengths after increased L6 activity.

(E) AMPAR- and NMDAR-mediated maximum EPSCs were not significantly altered in CNO-injected mice.

(F) The number of RGCs innervating each relay neuron was significantly larger after HM3Dq activation, as shown by the decreased fiber fraction.

For (C)–(F), box plots show interquartile range, whiskers show 10th and 90th percentiles. n = vehicle injected: 51 cells from 13 mice; CNO injected: 46 cells from 12 mice. *$p < 0.05$, **$p < 0.01$.

matching that occurs in cortex during the ocular dominance critical period (Wang et al., 2010). A feedforward model of circuit development would not necessarily preclude this form of tuning, but maintaining plasticity of retinal inputs into the phase when cortical function is maturing (and relaying feedback) may allow retinogeniculate connectivity to be optimized by visual processing that occurs in cortex. Recent work in mice has demonstrated that direction- and orientation-selective RGCs project to dLGN and that relay neurons also exhibit some direction and orientation selectivity (Huberman et al., 2009; Kim et al., 2010; Marshel et al., 2012; Piscopo et al., 2013; Scholl et al., 2013; Zhao et al., 2013). As corticothalamic-projecting cells in L6 are "exquisitely" tuned to orientation and direction (Vélez-Fort et al., 2014), feedback from L6 during the critical period could further influence which RGCs connect to a given relay neuron to optimize for these types of feature selectivity.

Interactions between Feedforward and Feedback Projections during Circuit Formation

In earlier phases of development in the visual system, there is a bidirectional interaction between retinogeniculate and corticogeniculate axons as they map to the dLGN. Enucleation of the eye or genetic reduction of RGCs alters the timing of corticothalamic innervation (Brooks et al., 2013; Seabrook et al., 2013), while RGC axons fail to project to the dLGN in mice that develop without a cortex (Shanks et al., 2016). In the superior colliculus, the retinal input instructs alignment of the feedback projection, as genetic duplication of the retinocollicular map leads to bifurcation of the corticocollicular projection (Triplett et al., 2009). This group also showed that when molecular cues that guide axon mapping are manipulated more subtly, topographical mapping in SC becomes variable. Notably, disruption of correlated retinal activity eliminates this

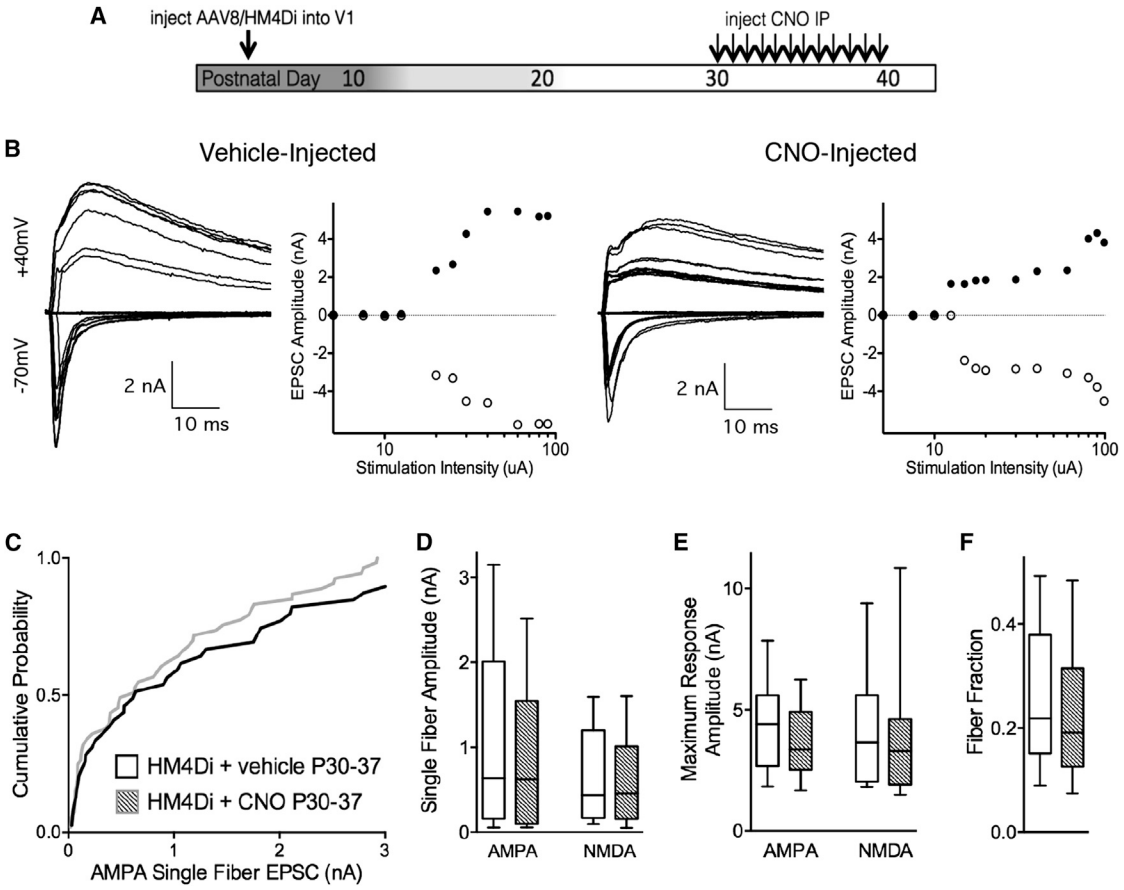

Figure 6. Suppressing Cortical Feedback Does Not Trigger Significant Retinogeniculate Remodeling in Older Mice

(A) Schematic of experimental design.

(B) Example recordings from relay neurons of vehicle- or CNO-injected mice.

(C–E) Distribution of AMPA single fiber strengths was similar in mice treated with vehicle or CNO (C). Both AMPA and NMDA single fiber strengths (D) and maximum EPSCs (E) did not significantly change with L6 inhibited from P30 to P37–P42.

(F) The number of retinal inputs converging onto each relay neuron was not significantly affected by altering cortical feedback after P30.

For (C)–(F), box plots show interquartile range, whiskers show 10th and 90th percentiles. n = vehicle injected: 21 cells from 9 mice; CNO injected: 35 cells from 11 mice.

stochasticity in mapping, supporting the idea that activity is able to redirect the final target of the retinotectal input away from that specified by molecular cues (Owens et al., 2015). Here we show that interactions during experience-dependent remodeling are also important, as cortical feedback to dLGN regulates the connectivity of retinal inputs onto relay neurons. Taken together with the previous studies, our studies highlight the importance of interactions between feedforward and feedback pathways, via precise activity patterns, in optimizing the final alignment of the mature circuit.

Mechanisms Underlying the Fine-Tuning of Feedforward Connections

The mechanisms underlying the interplay of cortical feedback and feedforward remodeling during critical period plasticity require further investigation, as corticothalamic neurons can both enhance relay neuron activity directly at synapses onto distal dendrites (through both ionotropic and metabotropic glutamate receptors) and inhibit relay neuron activity through disynaptic connections via the thalamic reticular nucleus (TRN) and local interneurons in the dLGN (see Figure 7). This can explain the increase in dLGN activity after L6 suppression by HM4Di (Figure 4), if relay neurons are ultimately disinhibited by this manipulation. The decrease in the number of relay neurons suppressed by visual stimulation (Figure 4C) might also result from the loss of L6-driven inhibition (although the rewiring of retinal inputs may also play a role here).

Furthermore, recent studies of this circuit have demonstrated that the corticothalamic influence on relay neuron activity involves a dynamic balance of excitatory and inhibitory drive, which, during trains of activity, shifts from a net inhibitory to a net excitatory influence due to short-term plasticity mechanisms in the circuit (Augustinaite et al., 2011; Crandall et al., 2015). This feature of the circuit may explain the different retinogeniculate phenotypes seen with muscimol and HM4DI, as the degree by which each manipulation reduces L6 spiking could lead to

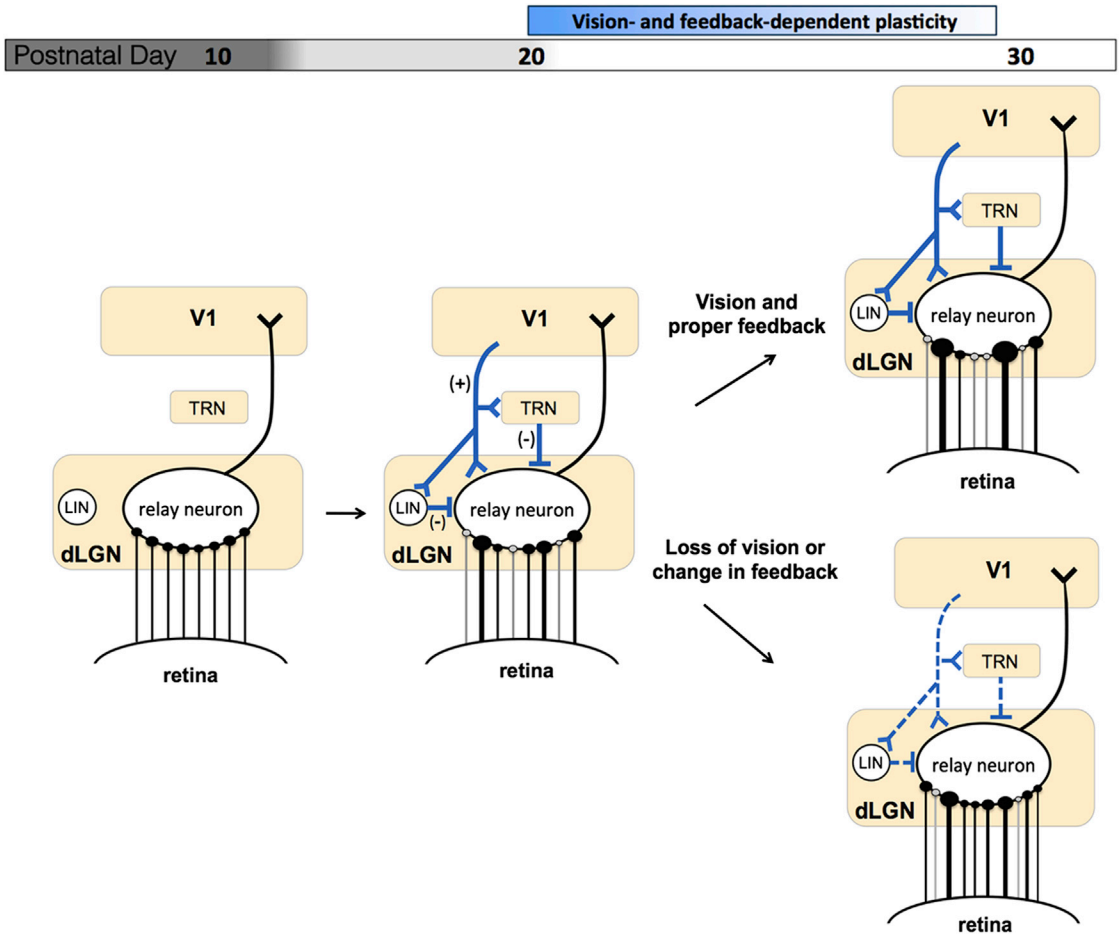

Figure 7. Revised Model for Retinogeniculate Refinement during Development

Thickness of lines and size of circles indicate the relative strength of RGC inputs onto relay neurons. At P10, retinal inputs to relay neurons are weak and numerous, and the cortical feedback circuit is not fully connected. By P20, many retinal inputs have been functionally eliminated (axon arbors remain present, indicated by gray contacts, but represent latent or extremely weak synapses), while others have strengthened. By this point, cortical feedback has begun to influence relay neuron activity, and thus drastic changes in cortical activity during the subsequent critical period (indicated by dashed lines in the bottom row at P30) disrupt the final stage of refinement. This leads to an increase rather than decrease in the number of functional inputs at P30, similar to the effect of visual deprivation during this stage of development. This phenotype is seen with all three perturbations of cortical activity reported here. In the case of HM4Di-manipulated L6 activity, relay neuron activity is elevated, leading to the strengthening of the newly recruited inputs.

significantly different shifts in this excitatory/inhibitory balance. The additional effect of HM4Di on corticothalamic short-term plasticity (Figure S2) (Stachniak et al., 2014) may also contribute to this difference. Thus, while both manipulations recruit new retinal inputs, in the case of inhibitory DREADDs, the increased activity of relay neurons would lead to those newly recruited inputs more readily strengthening through Hebbian mechanisms. Alternatively, as the activity of relay neurons' target cells in L4 increases with HM4Di (Figure 2G), but not with muscimol (Figure 1B), another possibility is that a retrograde signal in thalamocortical neurons influences the strengthening of retinal inputs based on downstream activity.

The Anatomical Basis for Changes in Connectivity

Regardless of the mechanism(s) influencing input strength, the distinct manipulations of cortical activity all result in a common phenotype, defined by a significant increase in the number of functional retinal inputs converging on each relay neuron. A morphological basis for this change in connectivity is suggested by recent anatomical findings from multiple groups. Visual deprivation during the thalamic critical period leads to a redistribution of boutons along a broad axon arbor rather than large-scale sprouting and retraction of axonal segments (Hong et al., 2014). Consistent with these findings, Morgan et al. (2016) recently showed that at P32, the number of RGC axons that make contact onto a given relay neuron is much greater than what is functionally detectable (see also Hammer et al., 2015). Therefore, our manipulations of cortical feedback could lead to the common intermediate state of connectivity by shifting the weights of synapses within this network, strengthening weak or latent synapses and weakening strong inputs, without having to drastically reshape retinal axonal arbors (Figure 7). During

normal development, the maintenance of broad axon scaffolds through the thalamic critical period may allow for the rapid revision of pre- and post-synaptic partners in order to fine tune connectivity according to cortically processed visual input.

Conclusion

It has been generally assumed that thalamic circuits mature and stabilize locally, well before their corresponding sensory cortical circuits undergo critical period plasticity. Our data show that changes originating in cortex can propagate back to thalamus and modify the primary afferent input onto relay cells. These changes will in turn alter thalamocortical output, further influencing cortical processing. Thus, the development of sensory pathways is not a hierarchical progression but entails a brief window for distant microcircuits to interact, process sensory input, and modify connections accordingly. Similar thalamic critical periods have been described for other sensory modalities as well (Wang and Zhang, 2008), also within developmental time frames overlapping with corresponding cortical plasticity. Therefore, feedback during development may be a common mechanism for fine tuning sensory circuits.

EXPERIMENTAL PROCEDURES

Animals

All animal procedures were in compliance with the NIH Guide for the Care and Use of Laboratory Animals and approved by the Institutional Animal and Care and Use Committee (IACUC) at Boston Children's Hospital. Transgenic lines were maintained on a C57/BL6 background. The NTSR1-Cre line was obtained via the Mutant Mouse Regional Resource Centers (MMRRC).

Viral Injections

AAVs were obtained from the UNC Viral Vector Core (rAAV8/hSyn-DIO-HM4D(G_i)-mCherry and rAAV8/hSyn-DIO-HM3D(G_q)-mCherry, titers > 10^{12} molecules/mL). Virus was injected into neonatal pups (P1–P2) anesthetized on ice and secured to a stereotax platform (Narishige). A sharp micropipette loaded onto a Narishige microinjector was used to penetrate the skull and inject each mouse with 200 nL of virus at two depths and at two medial-lateral sites in V1, at a rate of 20 nL/min. Weeks later, CNO was delivered intraperitoneally at a dose of 1 mg/kg to activate DREADD receptors.

Muscimol Injections

Muscimol (30 mM, Tocris) or vehicle control was injected (blinded) into juvenile pups after anesthesia by 2.0% isoflurane, using a stereotax. The skull above V1 was thinned using a dental drill, and a 27G syringe needle was used to make a small hole for either a Hamilton syringe or a sharp micropipette. Muscimol was injected at a rate of 50 nL/min to deliver 1 uL across two sites at a depth of 0.5–0.6 mm. Afterward, the scalp was sutured and the mouse injected subcutaneously with meloxicam (5 mg/kg) immediately after surgery and again 24 hr post-operation.

Slice Preparation

Mice were anesthetized using isoflurane and decapitated. The brain was quickly removed and submerged in ice-cold choline-based cutting solution containing (in mM) 110 choline chloride, 3.1 sodium pyruvate, 11.6 sodium ascorbate, 25 $NaHCO_3$, 25 D-glucose, 7 $MgCl_2$, 2.5 KCl, 1.25 NaH_2PO_4, 0.5 $CaCl_2$. LGN slices were cut using a sapphire blade (DDK) as previously described (Hooks and Chen, 2006). After cutting, slices were allowed to recover at 31°C for 10 min in the choline cutting solution and then for 20 min in saline solution (in mM: NaCl 125, $NaHCO_3$ 25, glucose 25, KCl 2.5, NaH_2PO_3 1.25, $MgCl_2$ 1, and $CaCl_2$ 2). Oxygenation (95% O_2/5% CO_2) was continuously supplied during cutting and recovery.

Electrophysiological Recordings

Whole-cell voltage clamp recordings of thalamic relay neurons in the contralateral monocular region of the dLGN were performed as described previously (Hooks and Chen, 2006). Briefly, glass electrodes of 1.2–2.0 MΩ resistance were filled with an internal solution of (in mM) CsF 35, CsCl 100, EGTA 10, HEPES 10 (pH 7.32) (with CsOH). D600 (0.1 mM; methoxyverapamil hydrochloride; Tocris) was added to block voltage-gated calcium channels. Slices were continuously perfused with oxygenated saline (in mM): NaCl 125, $NaHCO_3$ 25, glucose 25, KCl 2.5, NaH_2PO_3 1.25, $MgCl_2$ 1, and $CaCl_2$ 2, and the $GABA_A$ receptor antagonist bicuculline (20 uM, Tocris) to silence local inhibitory circuits. For recording corticothalamic EPSCs, the NMDA receptor antagonist CPP (10 μM, Tocris) was also added. Stimulation of the optic tract was effected using glass pipettes filled with saline, and moved along the optic tract to evoke the largest postsynaptic response, but never beyond the ventral-caudal corner of the vLGN so as to avoid stimulating corticothalamic inputs directly. Maximal currents were defined as the largest postsynaptic response elicited when increasing stimulation intensity up to 99 μA. Single fiber responses were defined as the first consistent EPSC observed after an increase in stimulation intensity of 0.25 μA. If a second input of greater than five times the amplitude of the first could be isolated, it was also included. Occasionally, the first response to emerge was weak (<50 pA) at +40 mV and accompanied by a small amplitude current with slow kinetics at −70 mV; these responses were excluded from analysis as they likely represent synaptic spillover (Hauser et al., 2014). Fiber fractions for each cell were computed for all single fibers obtained in this way and averaged to give a single value for each cell. For a detailed discussion of how single fibers were ascertained and fiber fractions were interpreted, see Supplemental Experimental Procedures of Noutel et al. (2011) and Hooks and Chen (2008), respectively.

Whole-cell current-clamp recordings to evaluate DREADD efficacy were performed on cortical slices cut in the coronal plane. L6 cells expressing DREADD constructs were targeted for recording via mCherry fluorescence, and recordings were carried out using glass pipettes (5–8 MΩ) and an internal solution consisting of (in mM) 116 $KMeSO_4$, 6 KCl, 2 NaCl, 20 HEPES, 0.5 EGTA, 4 MgATP, 0.3 NaGTP, 10 $NaPO_4$ creatine (pH 7.25), with KOH. After break-in, the amplitudes of a series of three current injections were quickly adjusted so as to elicit no or few spikes (threshold), a low-frequency response, or a high-frequency response. Then, baseline firing rates were collected for these levels (delivered at a frequency of 0.016 Hz) for 10 min, at which point CNO (10 μM, Sigma) was bath applied. To evaluate the effectiveness of DREADD activation, spiking rates were averaged from the five trials preceding CNO addition and compared with five consecutive trials 10 min after application of CNO.

In Vivo Single Unit Recordings

In vivo recordings were performed at P32–P35 after chronic treatment with vehicle or CNO from P20. The mice were anesthetized under urethane (0.8 g/kg, i.p.) / chlorprothixene (0.025 mg/kg, i.p.) using standard techniques (Niell and Stryker, 2008). Additionally, atropine (0.3 mg/kg) and dexamethasone (2 mg/kg) were administered subcutaneously to reduce secretions and edema, respectively. Cortical activity in the binocular zone of primary visual cortex was recorded using multichannel probes (A1 × 16–3 mm 50 −177, Neuronexus Technologies), and the signal was amplified, thresholded, and discriminated (SortClient, Plexon Technologies). Full-screen sine wave gratings (100% contrast, 0.03 cpd, 2 Hz) were presented on a screen (mean luminance = 32 cd/m^2). Orientations varying between 0° and 360° (12 steps, 30° spacing) were presented in random order (3 s each, 8 repeats). Evoked response was defined as the response at preferred orientation. A uniform gray screen of intermediate luminance was used to monitor spontaneous activity (3 s, 8 repeats). Based on their waveforms, we selected and analyzed only excitatory cells (Niell and Stryker, 2008). Single-unit isolation was ensured by analyzing the cell waveforms and discriminated on the basis of their individual characteristics (Offline Sorter, Plexon Technologies). Activity analysis was done using Matlab via SigTOOL (Lidierth, 2009). Only cells with a maximal evoked response > 0.3 spike/s were kept in the analysis to exclude neurons with weak visual responses. We found the recordings were stable over time in saline-injected mice.

Laminar location was evaluated with contrast-reversing square checkerboard (0.04 cpd, square-wave reversing at 0.5 or 1 Hz, 25–50 repeats). For the local field potential (LFP) recordings, extracellular signal was filtered from 1 to 300 Hz and sampled at 1.5 kHz. Current source density (CSD) was computed from the average LFP as previously described (Niell and Stryker, 2008) and using the CSD plotter toolbox. For the recordings in the LGN, full-screen sine wave gratings (100% contrast, 0.035 cpd, 3.2 Hz) were presented on the screen (mean luminance = 32 cd/m^2). Orientations varying between 0° and 360° (8 steps, 45° spacing) were presented in random order (1.5 s each, 8–10 repeats). A screen of intermediate luminance was used to monitor spontaneous activity (1.5 s, 8–10 repeats). We note here that this stimulation protocol was not optimized for distinguishing ON-responsive from OFF-responsive relay neurons but does allow for classification of cells as excited by visual stimulation or suppressed by visual stimulation.

Tissue Preparation and Immunohistochemistry

To assess muscimol efficacy, mice were dark-reared overnight and then exposed to ambient light for 1 hr prior to perfusion. Mice were administered a lethal dose of pentobarbital (180 mg/kg) via intraperitoneal injection and then transcardially perfused with ice-cold 0.1 M PBS followed by paraformaldehyde (PFA, 4% w/v). Afterward, brains were dissected out and post-fixed overnight at 4°C in 4% PFA. For assessing the efficiency of viral injections, brains were sectioned in the coronal plane at 50 μm using a vibrating microtome (Leica). For immunohistochemistry, brains were exposed to a sucrose gradient (up to 30% w/v) over 2 days and then sectioned in ice-cold PBS at 50 μm on the vibratome. After permeabilization and blocking in PBS with 1% Triton X-100 and 10% normal goat serum, c-*fos* primary antibody was applied (1:1,000, Cell Signaling, RRID: AB_2106617) overnight at room temperature. After washing, secondary antibody (1:1,000, anti-rabbit Alexa-Fluor 488, Life Technologies) was applied for 2 hr at room temperature. Sections were again washed and then mounted on slides for imaging. To quantify and statistically compare c-*fos* immunostaining intensity after different manipulations, fluorescence was always compared internally to the non-manipulated hemisphere.

Statistical Analysis

Datasets were first analyzed using the Kolmogorov-Smirnov test for normality. For nonparametric distributions of data, a Mann-Whitney test was used for comparison, whereas for normally distributed datasets a Student's t test was used. For comparing firing rates or resting membrane potentials before and after CNO application to assess DREADD efficacy, a pairwise t test was performed. For the single unit recordings, the effect of the drug over time was analyzed using Friedman test with Dunn's multiple comparison. In all figures, *$p < 0.05$, **$p < 0.01$, ***$p < 0.001$.

SUPPLEMENTAL INFORMATION

Supplemental Information includes six figures and one table and can be found with this article online at http://dx.doi.org/10.1016/j.neuron.2016.07.040.

AUTHOR CONTRIBUTIONS

A.D.T., C.C., N.P., and M.F. designed the study. N.P. performed and analyzed in vivo physiological recordings, L.M. performed muscimol injections, and A.D.T. performed all other experiments and analysis. A.D.T. and C.C. wrote the manuscript.

ACKNOWLEDGMENTS

The authors thank E. Litvina and J. Hauser for helpful discussions on the experiments and manuscript and S. Park, J. Leffler, and E. Kang for technical assistance. We also thank W. Regehr, R. Wilson, G. Kreiman, R. Born, T. Schwarz, L. Liang, T. Hensch, and L. Cheadle for comments on the manuscript. We thank the MMRRC for providing the NTSR1-Cre mouse line and B.M. Hooks, K. Svoboda, and S. Datta for assistance in obtaining this line and T. Hensch for use of his in vivo rig. We thank T. Hill and the FM Kirby Neurobiology Imaging Core for assistance with obtaining images. Finally, we thank Dr. Kush Kapur for his guidance on statistical testing. This work was supported by the NIH (R01EY013613) to C.C., NIH RO1NS070300, the Simons Foundation (SFAR1205440) and P30OHD018655 to C.C. and M.F., support from Pfizer to T. Hensch (for N.P.), and an NIH F31 (5F31NS083437-03) to A.D.T.

Received: November 12, 2015
Revised: June 8, 2016
Accepted: July 8, 2016
Published: August 18, 2016

REFERENCES

Ackman, J.B., Burbridge, T.J., and Crair, M.C. (2012). Retinal waves coordinate patterned activity throughout the developing visual system. Nature *490*, 219–225.

Alexander, G.M., Rogan, S.C., Abbas, A.I., Armbruster, B.N., Pei, Y., Allen, J.A., Nonneman, R.J., Hartmann, J., Moy, S.S., Nicolelis, M.A., et al. (2009). Remote control of neuronal activity in transgenic mice expressing evolved G protein-coupled receptors. Neuron *63*, 27–39.

Armbruster, B.N., Li, X., Pausch, M.H., Herlitze, S., and Roth, B.L. (2007). Evolving the lock to fit the key to create a family of G protein-coupled receptors potently activated by an inert ligand. Proc. Natl. Acad. Sci. USA *104*, 5163–5168.

Augustinaite, S., Yanagawa, Y., and Heggelund, P. (2011). Cortical feedback regulation of input to visual cortex: role of intrageniculate interneurons. J. Physiol. *589*, 2963–2977.

Bortone, D.S., Olsen, S.R., and Scanziani, M. (2014). Translaminar inhibitory cells recruited by layer 6 corticothalamic neurons suppress visual cortex. Neuron *82*, 474–485.

Briggs, F., and Usrey, W.M. (2008). Emerging views of corticothalamic function. Curr. Opin. Neurobiol. *18*, 403–407.

Brooks, J.M., Su, J., Levy, C., Wang, J.S., Seabrook, T.A., Guido, W., and Fox, M.A. (2013). A molecular mechanism regulating the timing of corticogeniculate innervation. Cell Rep. *5*, 573–581.

Chen, C., and Regehr, W.G. (2000). Developmental remodeling of the retinogeniculate synapse. Neuron *28*, 955–966.

Crandall, S.R., Cruikshank, S.J., and Connors, B.W. (2015). A corticothalamic switch: controlling the thalamus with dynamic synapses. Neuron *86*, 768–782.

Cudeiro, J., and Sillito, A.M. (2006). Looking back: corticothalamic feedback and early visual processing. Trends Neurosci. *29*, 298–306.

Dunn, F.A., Della Santina, L., Parker, E.D., and Wong, R.O.L. (2013). Sensory experience shapes the development of the visual system's first synapse. Neuron *80*, 1159–1166.

Fagiolini, M., Pizzorusso, T., Berardi, N., Domenici, L., and Maffei, L. (1994). Functional postnatal development of the rat primary visual cortex and the role of visual experience: dark rearing and monocular deprivation. Vision Res. *34*, 709–720.

Gong, S., Doughty, M., Harbaugh, C.R., Cummins, A., Hatten, M.E., Heintz, N., and Gerfen, C.R. (2007). Targeting Cre recombinase to specific neuron populations with bacterial artificial chromosome constructs. J. Neurosci. *27*, 9817–9823.

Gordon, J.A., and Stryker, M.P. (1996). Experience-dependent plasticity of binocular responses in the primary visual cortex of the mouse. J. Neurosci. *16*, 3274–3286.

Guillery, R.W., and Sherman, S.M. (2002). Thalamic relay functions and their role in corticocortical communication: generalizations from the visual system. Neuron *33*, 163–175.

Hammer, S., Monavarfeshani, A., Lemon, T., Su, J., and Fox, M.A. (2015). Multiple Retinal Axons Converge onto Relay Cells in the Adult Mouse Thalamus. Cell Rep. *12*, 1575–1583.

Hauser, J.L., Liu, X., Litvina, E.Y., and Chen, C. (2014). Prolonged synaptic currents increase relay neuron firing at the developing retinogeniculate synapse. J. Neurophysiol. *112*, 1714–1728.

Hong, Y.K., and Chen, C. (2011). Wiring and rewiring of the retinogeniculate synapse. Curr. Opin. Neurobiol. *21*, 228–237.

Hong, Y.K., Park, S., Litvina, E.Y., Morales, J., Sanes, J.R., and Chen, C. (2014). Refinement of the retinogeniculate synapse by bouton clustering. Neuron *84*, 332–339.

Hooks, B.M., and Chen, C. (2006). Distinct roles for spontaneous and visual activity in remodeling of the retinogeniculate synapse. Neuron *52*, 281–291.

Hooks, B.M., and Chen, C. (2008). Vision triggers an experience-dependent sensitive period at the retinogeniculate synapse. J. Neurosci. *28*, 4807–4817.

Huberman, A.D., Feller, M.B., and Chapman, B. (2008). Mechanisms underlying development of visual maps and receptive fields. Annu. Rev. Neurosci. *31*, 479–509.

Huberman, A.D., Wei, W., Elstrott, J., Stafford, B.K., Feller, M.B., and Barres, B.A. (2009). Genetic identification of an On-Off direction-selective retinal ganglion cell subtype reveals a layer-specific subcortical map of posterior motion. Neuron *62*, 327–334.

Jacobs, E.C., Campagnoni, C., Kampf, K., Reyes, S.D., Kalra, V., Handley, V., Xie, Y.Y., Hong-Hu, Y., Spreur, V., Fisher, R.S., and Campagnoni, A.T. (2007). Visualization of corticofugal projections during early cortical development in a tau-GFP-transgenic mouse. Eur. J. Neurosci. *25*, 17–30.

Jurgens, C.W.D., Bell, K.A., McQuiston, A.R., and Guido, W. (2012). Optogenetic stimulation of the corticothalamic pathway affects relay cells and GABAergic neurons differently in the mouse visual thalamus. PLoS ONE *7*, e45717.

Kang, E., Durand, S., LeBlanc, J.J., Hensch, T.K., Chen, C., and Fagiolini, M. (2013). Visual acuity development and plasticity in the absence of sensory experience. J. Neurosci. *33*, 17789–17796.

Katz, L.C., and Shatz, C.J. (1996). Synaptic activity and the construction of cortical circuits. Science *274*, 1133–1138.

Kim, I.-J., Zhang, Y., Meister, M., and Sanes, J.R. (2010). Laminar restriction of retinal ganglion cell dendrites and axons: subtype-specific developmental patterns revealed with transgenic markers. J. Neurosci. *30*, 1452–1462.

Lidierth, M. (2009). sigTOOL: A MATLAB-based environment for sharing laboratory-developed software to analyze biological signals. J. Neurosci. Methods *178*, 188–196.

Lin, D.J.-P., Kang, E., and Chen, C. (2014). Changes in input strength and number are driven by distinct mechanisms at the retinogeniculate synapse. J. Neurophysiol. *112*, 942–950.

Marshel, J.H., Kaye, A.P., Nauhaus, I., and Callaway, E.M. (2012). Anterior-posterior direction opponency in the superficial mouse lateral geniculate nucleus. Neuron *76*, 713–720.

Montero, V.M. (1991). A quantitative study of synaptic contacts on interneurons and relay cells of the cat lateral geniculate nucleus. Exp. Brain Res. *86*, 257–270.

Morgan, J.L., Berger, D.R., Wetzel, A.W., and Lichtman, J.W. (2016). The Fuzzy Logic of Network Connectivity in Mouse Visual Thalamus. Cell *165*, 192–206.

Murphy, P.C., and Sillito, A.M. (1996). Functional morphology of the feedback pathway from area 17 of the cat visual cortex to the lateral geniculate nucleus. J. Neurosci. *16*, 1180–1192.

Niell, C.M., and Stryker, M.P. (2008). Highly selective receptive fields in mouse visual cortex. J. Neurosci. *28*, 7520–7536.

Noutel, J., Hong, Y.K., Leu, B., Kang, E., and Chen, C. (2011). Experience-dependent retinogeniculate synapse remodeling is abnormal in MeCP2-deficient mice. Neuron *70*, 35–42.

Olsen, S.R., Bortone, D.S., Adesnik, H., and Scanziani, M. (2012). Gain control by layer six in cortical circuits of vision. Nature *483*, 47–52.

Owens, M.T., Feldheim, D.A., Stryker, M.P., and Triplett, J.W. (2015). Stochastic Interaction between Neural Activity and Molecular Cues in the Formation of Topographic Maps. Neuron *87*, 1261–1273.

Piscopo, D.M., El-Danaf, R.N., Huberman, A.D., and Niell, C.M. (2013). Diverse visual features encoded in mouse lateral geniculate nucleus. J. Neurosci. *33*, 4642–4656.

Scholl, B., Tan, A.Y.Y., Corey, J., and Priebe, N.J. (2013). Emergence of orientation selectivity in the Mammalian visual pathway. J. Neurosci. *33*, 10616–10624.

Seabrook, T.A., El-Danaf, R.N., Krahe, T.E., Fox, M.A., and Guido, W. (2013). Retinal input regulates the timing of corticogeniculate innervation. J. Neurosci. *33*, 10085–10097.

Shanks, J.A., Ito, S., Schaevitz, L., Yamada, J., Chen, B., Litke, A., and Feldheim, D.A. (2016). Corticothalamic Axons Are Essential for Retinal Ganglion Cell Axon Targeting to the Mouse Dorsal Lateral Geniculate Nucleus. J. Neurosci. *36*, 5252–5263.

Shatz, C.J., and Rakic, P. (1981). The genesis of efferent connections from the visual cortex of the fetal rhesus monkey. J. Comp. Neurol. *196*, 287–307.

Sillito, A.M., Jones, H.E., Gerstein, G.L., and West, D.C. (1994). Feature-linked synchronization of thalamic relay cell firing induced by feedback from the visual cortex. Nature *369*, 479–482.

Sretavan, D., and Shatz, C.J. (1984). Prenatal development of individual retinogeniculate axons during the period of segregation. Nature *308*, 845–848.

Stachniak, T.J., Ghosh, A., and Sternson, S.M. (2014). Chemogenetic synaptic silencing of neural circuits localizes a hypothalamus→midbrain pathway for feeding behavior. Neuron *82*, 797–808.

Temereanca, S., and Simons, D.J. (2004). Functional topography of corticothalamic feedback enhances thalamic spatial response tuning in the somatosensory whisker/barrel system. Neuron *41*, 639–651.

Tian, N., and Copenhagen, D.R. (2003). Visual stimulation is required for refinement of ON and OFF pathways in postnatal retina. Neuron *39*, 85–96.

Triplett, J.W., Owens, M.T., Yamada, J., Lemke, G., Cang, J., Stryker, M.P., and Feldheim, D.A. (2009). Retinal input instructs alignment of visual topographic maps. Cell *139*, 175–185.

Vélez-Fort, M., Rousseau, C.V., Niedworok, C.J., Wickersham, I.R., Rancz, E.A., Brown, A.P.Y., Strom, M., and Margrie, T.W. (2014). The stimulus selectivity and connectivity of layer six principal cells reveals cortical microcircuits underlying visual processing. Neuron *83*, 1431–1443.

Wang, H., and Zhang, Z.W. (2008). A critical window for experience-dependent plasticity at whisker sensory relay synapse in the thalamus. J. Neurosci. *28*, 13621–13628.

Wang, W., Jones, H.E., Andolina, I.M., Salt, T.E., and Sillito, A.M. (2006). Functional alignment of feedback effects from visual cortex to thalamus. Nat. Neurosci. *9*, 1330–1336.

Wang, B.S., Sarnaik, R., and Cang, J. (2010). Critical period plasticity matches binocular orientation preference in the visual cortex. Neuron *65*, 246–256.

Wiesel, T.N., and Hubel, D.H. (1963). Single-Cell Responses in Striate Cortex of Kittens Deprived of Vision in One Eye. J. Neurophysiol. *26*, 1003–1017.

Zhao, X., Chen, H., Liu, X., and Cang, J. (2013). Orientation-selective responses in the mouse lateral geniculate nucleus. J. Neurosci. *33*, 12751–12763.